Increasing Upconversion by Plasmon Resonance in Metal Nanoparticles—A Combined Simulation Analysis

J. C. Goldschmidt, S. Fischer, H. Steinkemper, F. Hallermann, G. von Plessen, K. W. Krämer, D. Biner, and M. Hermle

Abstract—Upconversion (UC) of subbandgap photons has the potential to increase solar cell efficiencies. In this paper, we first review our recent investigations of silicon solar cell devices with an attached upconverter based on β-NaYF$_4$:20%Er^{3+}. Such devices showed peak external quantum efficiencies of 0.64% under monochromatic excitation at 1523 nm and an irradiance of 2305 Wm^{-2}. Under broad spectrum illumination, an average UC efficiency of 1.07 ± 0.13% in the spectral range from 1460 to 1600 nm was achieved. The measured quantum efficiency corresponds to a relative efficiency increase of 0.014% for the used bifacial silicon solar cell with 16.70% overall efficiency. This increase is too small to make UC relevant in photovoltaics. Therefore, additional means of increasing the UC efficiency are necessary. In this paper, we investigate plasmon resonance in metal nanoparticles in the proximity of the UC material, with the aim of increasing UC efficiency. The local field enhancement by the plasmon resonance positively influences UC efficiency because of the nonlinear nature of UC. Additionally, the metal nanoparticles also influence the transition probabilities in the upconverter. To investigate the effects, we combine different simulation models. We use a rate equation model to describe the UC dynamics in β-NaYF$_4$:20%Er^{3+}. The model considers ground state and excited state absorption, spontaneous and stimulated emission, energy transfer, and multiphonon decay. The rate equation model is coupled with Mie theory calculations of the changed optical field in the proximity of a gold nanoparticle. The changes of the transition rates both for radiative and nonradiative processes are calculated with exact electrodynamic theory. Calculations are performed in high resolution for a 3-D simulation volume. The results suggest that metal nanoparticles can increase UC efficiency.

Index Terms—Erbium, nanophotonics, photovoltaic cells, upconversion (UC).

J. C. Goldschmidt, S. Fischer, H. Steinkemper, and M. Hermle are with the Fraunhofer Institute for Solar Energy Systems ISE, 79110 Freiburg, Germany (e-mail: jan.christoph.goldschmidt@ise.fraunhofer.de; stefan.fischer@ise.fraunhofer.de; heiko.steinkemper@ise.fraunhofer.de; martin.hermle@ise.fraunhofer.de).

F. Hallermann and G. von Plessen are with the Institute of Physics (1A), RWTH Aachen, 52056 Aachen, Germany (e-mail: Hallermann@physik.rwth-aachen.de; gero.vonplessen@rwth-aachen.de).

K. W. Krämer and D. Biner are with the Department of Chemistry, University of Bern, 3012 Bern, Switzerland (e-mail: karl.kraemer@iac.unibe.ch; daniel.biner@iac.unibe.ch).

Color versions of one or more of the figures in this paper are available online at http://ieeexplore.ieee.org.

Digital Object Identifier 10.1109/JPHOTOV.2011.2182179

I. INTRODUCTION

SILICON solar cells lose about 20% of the energy incident from the sun, because subbandgap photons are transmitted. Upconversion (UC) aims to reduce these losses by converting two subbandgap photons into one photon with an energy above the bandgap [1], [2]. Trivalent erbium-doped hexagonal sodium yttrium fluoride (β-NaYF4:20% Er^{3+}) is a very suitable UC material that shows high UC quantum yield and emission/absorption characteristics that match the spectral characteristic of silicon solar cells [3]–[6]. In Section II, we will review the results achieved recently with this UC material. As we will see, the results indicate that additional means are necessary to increase UC efficiency.

One option is to utilize the plasmon resonance of metal nanoparticles in the proximity of the UC material. The higher local field intensities caused by the plasmon resonance positively influence UC efficiency because of the nonlinear nature of UC. Additionally, the metal nanoparticles also influence the transition probabilities of the luminescent system [7]–[10]. Such plasmonic effects have been investigated intensively [11]–[16]. For Er^{3+}, Mertens and Polman [12] demonstrated an increase of the photoluminescence by more than a factor of two, when Er^{3+} were located in the proximity of an array of elongated Ag nanoparticles. Schietinger *et al.* [14] demonstrated a 3.8-fold increase in UC luminescence, when a NaYF$_4$ nanocrystal codoped with Yb^{3+}/Er^{3+} was placed at an optimized position near a gold nanosphere with 60-nm diameter. Schietinger *et al.* found that the observed increase was more pronounced than expected from a theoretical model that described UC with rate equations for a simple three-level system and was presented by Esteban *et al.* [17]. In Section III, we present a more complex model for the UC system of β-NaYF4:20%Er^{3+} that describes the UC dynamics more precisely. In Section IV, we show how this UC model is coupled to simulations of plasmon resonance in gold nanoparticles. The impact of a gold nanoparticle on the UC is then analyzed in detail.

II. DEVICE MEASUREMENTS

A powder of the UC material β-NaYF$_4$:20%Er^{3+} was mixed with the binding agent zapon varnish 79550—Zapon Lacquer

and attached to the grid-free side of a bifacial, back-junction silicon solar cell with an active area of 4.5 mm × 4.5 mm. The placement of the upconverter at the grid-free side of the solar cell avoids problems with the contacts of the solar cell, but results in shading losses. Hence, this is not a configuration to reach highest efficiencies, but provides a convenient test device. Under 1-sun AM1.5G illumination on the grid-covered side, the solar cell exhibits 16.7% efficiency [6].

For the measurement of the external quantum efficiency (EQE), the solar cell was placed on a cooled gold-coated measurement chuck, which has a cavity for the upconverter. The solar cell UC system was illuminated with a Santec ECL-210 laser from the grid-covered side. The wavelength of the laser λ_{inc} can be tuned from 1430 to 1630 nm and the irradiance on the sample I can be tuned up to 2305 Wm^{-2}. The EQE increases with the irradiance because of the nonlinear nature of the UC involving at least two photons [1]. The highest EQE was measured at a wavelength of 1523 nm, reaching 0.64% for an irradiance of 2305 Wm^{-2}. Extrapolations of these results agree very well with other studies [4], on the same material β-NaYF$_4$:20%Er^{3+}, and constitute the highest UC efficiencies achieved in the context of silicon solar cells, when the relatively low irradiance values are taken into account [5], [6].

The application of UC to harvest solar energy implies that the upconverter operates under broad spectrum illumination and not under monochromatic laser excitation. Therefore, we investigated the described UC solar cell device also under the light of a Xe-lamp concentrated by lenses onto the device [6]. A polished Si wafer served as a long-pass filter to increase the relative impact of the upconverter. By comparison of the short-circuit current measured with UC material attached to the solar cell, to the case where a polytetrafluoroethylene reflector was attached instead, it was ensured that any measured effect was due to UC. We observed a significant current due to UC, which corresponds to an average UC efficiency of $1.07 \pm 0.13\%$ in the spectral range from 1460 to 1600 nm. The photon flux in this spectral range corresponded to an effective concentration of 732 ± 17 sun. It is interesting to note that the observed average EQE is higher than the peak values of the EQE determined under monochromatic illumination with comparable irradiance levels. This is attributed to the resonant excitation of the two most important optical transitions under broad spectrum illumination, which is not the case under monochromatic illumination. The measured quantum efficiency corresponds to a relative efficiency increase of 0.014% for the used bifacial silicon solar cell with its 16.70% overall efficiency. This increase is too small to make UC relevant in photovoltaics. Therefore, additional means of increasing UC efficiency are necessary, e.g., the use of plasmon resonance in metal nanoparticles.

III. SIMULATING UPCONVERSION WITH A RATE EQUATION MODEL

A. Model

The UC dynamics of β-NaYF$_4$:20%Er^{3+} were modeled by rate equations [18]. The model considers ground and excited state absorption, spontaneous and stimulated emission, energy
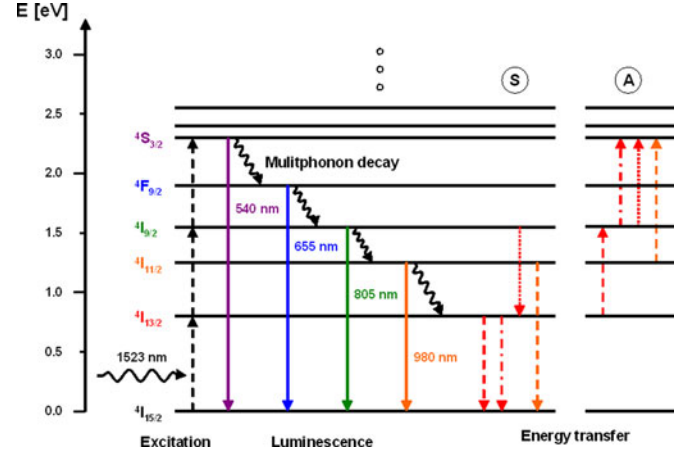

Fig. 1. Energy levels of Er^{3+} in the host crystal β-NaYF$_4$ with corresponding luminescence wavelengths of the photoluminescence transitions from the excited states to the ground state (solid arrows). In the rate equation model excitation with 1523 nm is assumed. Higher energy levels are populated by ground and excited state absorption (black-dashed arrows). Additionally, energy transfer occurs, where energy is transferred from the sensitizer ion (S), to the activator ion (A) (dashed and pointed arrows). Furthermore, multiphonon relaxation between neighboring energy levels is considered (waved arrows).

transfer, and multiphonon relaxation. The considered transitions and energy levels are shown in Fig. 1. The most important input parameters of the model are the Einstein coefficients of the involved radiative transitions. They were derived from absorption coefficient data of the β-NaYF$_4$:20%Er^{3+} powder using the theory of Judd [19] and Ofelt [20]. Other parameters, such as the values of the overlap integrals describing the energy transfer, were estimated based on literature data [21]. The parameters describing multiphonon relaxation were estimated from literature values of similar materials [22] and adjusted to achieve good agreement between simulation and measurement. More details on the rate equation model can be found in [18] and [23].

B. Comparison Between Model and Experimental Data

For photoluminescence measurements, the β-NaYF4: 20%Er^{3+} powder was illuminated at a wavelength of 1523 nm with an IR-Laser ECL-210 from Santec. The luminescence spectra were recorded with a grating monochromator H25 from Jobin Yvon, a silicon photodiode detector from OptoElectronic Components, and a lock-in-amplifier 7265 from Signal Recovery. The setup was calibrated [5]; therefore, it was possible to determine the UC quantum yield η_{UC}. For this purpose, the number of photons emitted with energies above the bandgap of silicon was divided by the number of photons incident on the powder cell. Fig. 2 shows how the UC quantum yield increases with increasing irradiance. The sum of the spontaneous emission rates of photons with energies above the bandgap of silicon was divided by the sum of the ground and excited state absorption rates subtracted by the stimulated emission rate. This quantity represents the simulated internal UC quantum yield and can be compared with the UC quantum yield η_{UC} from the
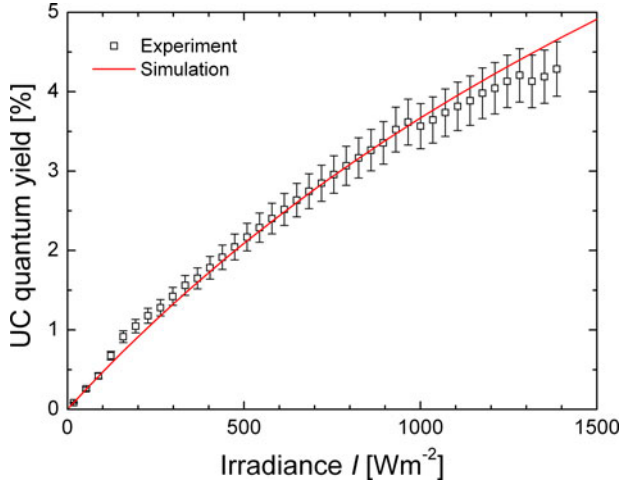
Fig. 2.   Comparison of the measured and simulated UC quantum yield. The agreement between model and measurement is very good.

Fig. 3.   Enhancement factor of the quadratic electric field γ_E due to a spherical gold nanoparticle with a diameter of 200 nm (white circle in the center) at an illumination with wavelength of 1523 nm. The plot shows a cut through the simulation volume in the xz plane at $y = 0$ nm. The incident light propagates in the positive z-direction from the bottom of the graph. The strongest field enhancement with a value of $\gamma_E = 16$ is reached close to the surface of the gold nanoparticle.

experiments. Fig. 2 shows that the model describes the dependence of the UC yield on the irradiance very well.

IV. SIMULATING THE IMPACT OF THE PLASMON RESONANCE IN METAL NANOPARTICLES ON UPCONVERSION

A. Coupling of Nanoparticle Simulation and Rate Equation Model

The plasmon resonance in metal nanoparticles alters the field intensity around the particles. Because of the nonlinear characteristic of the UC process (see Fig. 2), the locally increased field intensities can be used to increase the UC efficiency. Furthermore, coupling effects influence the transition probabilities for wanted and unwanted transitions in the upconverter. These effects were simulated for a cubic volume with one spherical gold nanoparticle in the center. The edge length of the simulation volume was six times the diameter of the nanoparticle. The resolution of the simulation was 5 nm. Details on the simulation approach can be found in [24].

Because of the high computational cost of a complete analysis, only the change of the intensity of the electric field was considered in a first run. We calculated the intensity distribution around gold nanoparticles with diameters from 40 to 480 nm for illumination with 1523 nm using Mie theory [25]. The resulting different levels of irradiance were used as input parameters for the UC rate equation model. It was found that for a particle diameter of 200 nm, the increase in UC luminescence due to the field enhancement effect was the largest [24].

In a second step, we calculated how the radiative and nonradiative transition probabilities within the upconverter are changed in the proximity of a particle with a diameter of 200 nm. We used exact electrodynamic theory [26]–[28] for this purpose. The theory is based on Mie theory, which provides solutions to Maxwell's equations for spherical boundary conditions. The theoretical model is implemented in MATLAB; details can be found in [13]. The relative change of the Einstein coefficients, which describe the transitions used in the rate equation model, is calculated by the enhancement factor $\gamma_{\mathrm{tot},if}$ for a certain tran-
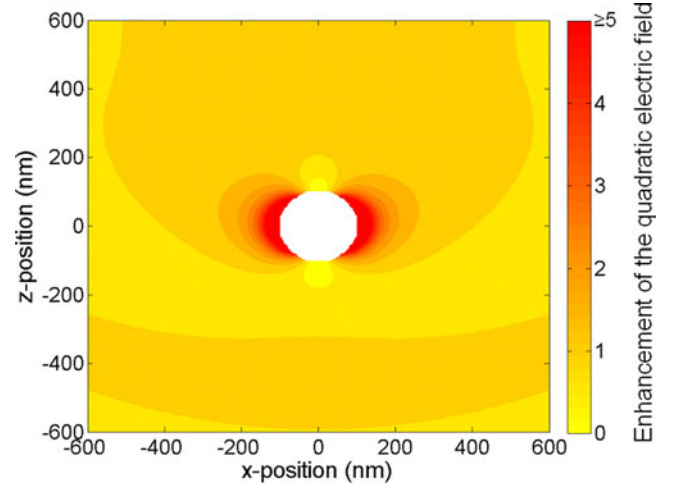
sition from energy level i to energy level f. The $\gamma_{\mathrm{tot},if}$ consist of a radiative factor $\gamma_{\mathrm{rad},if}$ for emitted photons and a nonradiative factor $\gamma_{\mathrm{nrad},if}$ for transition in which the excitation energy is lost due to energy transfer to the metal nanoparticle. Therefore, the $\gamma_{\mathrm{rad},if}$ was used to calculate the luminescence of the upconverter.

In the exact electrodynamic theory, the upconverter is treated as dipole emitter. The emitting dipole can be oriented in two different polarization directions with respect to the surface of the gold nanoparticle, either parallel to the surface (PPOL) or perpendicular to the surface (SPOL). In consequence, the different factors must be calculated for every polarization. The changed transition probabilities and the changed irradiance were used to calculate the UC luminescence at every point in the volume around the particle for each polarization.

B. Results

Fig. 3 shows the factor γ_E by which the quadratic electric field changes due to a spherical gold nanoparticle with a diameter of 200 nm under an illumination at a wavelength of 1523 nm. The plot shows a cut through the simulation volume in the xz plane at $y = 0$ nm. The incident light propagates in positive z-direction from the bottom of the graph. In the direction perpendicular to the light path, a very high field enhancement occurs, with γ_E values up to 16 close to the surface of the gold nanoparticle. Behind and in front of the nanoparticle, regions occur in which the field is decreased. For most of the simulated volume, the γ_E values are roughly one, indicating a marginal impact of the nanoparticle.

Fig. 4(a) and (b) shows how the rates for the different radiative transition depend on the distance from the nanoparticle for PPOL and SPOL polarization directions. For SPOL [see Fig. 4(b)], nearly all transitions show a significant increase,
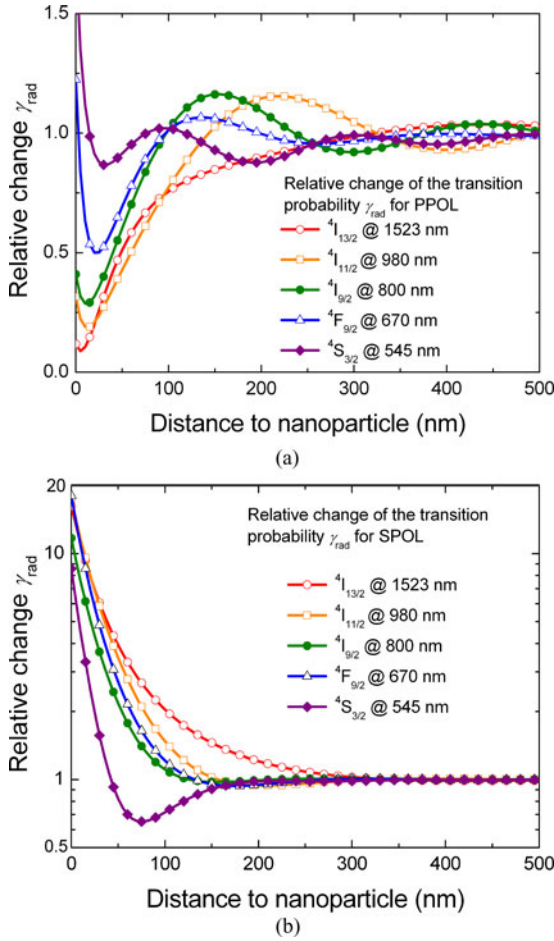
Fig. 4. Factor $\gamma_{\mathrm{rad},i}$ that describes the relative change of the radiative transition probabilities for (a) PPOL and (b) SPOL.
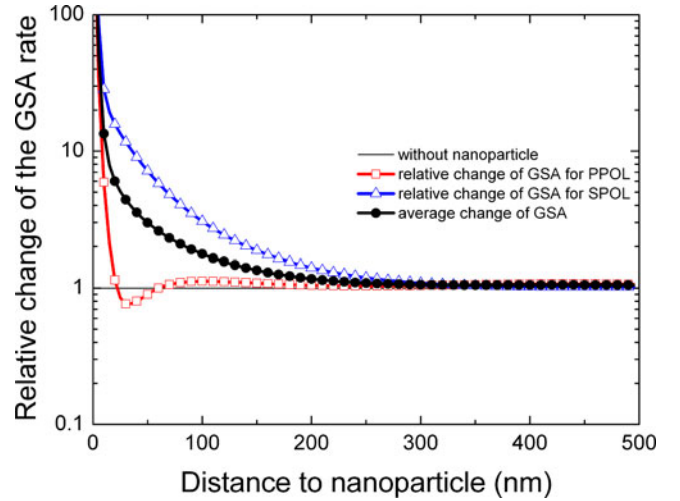

Fig. 5. Relative change of the ground state absorption (GSA) rate for PPOL and SPOL. The average takes the likelihood of the two polarizations into account. It can be seen that overall GSA increases, especially close to the nanoparticle.

which is stronger close to the nanoparticle. The most important transitions are the transition from $^4I_{13/2}$ and $^4I_{11/2}$ to the ground state $^4I_{15/2}$. The change of the radiative transition from $^4I_{13/2}$ to $^4I_{15/2}$ also affects the excitation. Hence, an increased probability of UC due to a higher occupation of the intermediate energy level $^4I_{13/2}$ is possible. The transition from $^4I_{11/2}$ to $^4I_{15/2}$ is the most important transition for UC luminescence. Depending on the irradiance, more than 95% of the UC luminescence originate from this transition [5]. These two transitions are modified individually depending on the distance to the nanoparticle. Enhancement factors greater than 5 are achieved for distances shorter than 50 nm for SPOL. For PPOL, enhancement and reduction is observed for the different transitions, while the mentioned most important transitions actually show a strong damping at 100 nm or closer to the nanoparticle.

Fig. 5 shows the change of the ground state absorption, resulting from the changes in the optical field and the changes in the transition rates. The average takes into account that PPOL is twice as likely as SPOL because there are two independent possibilities for an orientation of the dipole parallel to the surface of the gold nanoparticle. It can be seen that overall absorption increases, but close to the surface, the strong absorption is

caused by the strong nonradiative enhancement and lost to the nanoparticle.

Fig. 6(a) and (b) depicts the changes in the nonradiative processes. Quite independently from the polarization, it can be stated that nonradiative processes are strongly enhanced in a region of about 50 nm around the nanoparticle, while only little additional nonradiative recombination occurs further away from the particle.

Fig. 7(a) and (b) shows the overall changes in UC luminescence for the dominant transition from $^4I_{11/2}$ to $^4I_{15/2}$ when all the described effects are taken into account. Like in Fig. 3, the plot shows a cut through the simulation volume in the *xz* plane at $y = 0$ nm. The incident light propagates in positive *z*-direction from the bottom of the graph. A strong increase in UC luminescence is observed for SPOL as well as for PPOL around the gold nanoparticle, but a decrease is observed for PPOL for certain areas.

Fig. 8 depicts the changes of all transitions showing UC luminescence in dependence on the distance to the nanoparticle. These data were obtained by integration over spherical shells around the gold nanoparticle. At distances around 30 nm, a high increase in UC luminescence occurs. The increase is more pronounced for the higher energy transitions, reaching enhancement factors of up to 1000. For the most important emission from $^4I_{11/2}$ to $^4I_{15/2}$, an increase of UC luminescence of up to 17 was calculated at a distance of 25 nm.

It is interesting to investigate whether the increase in UC luminescence is a result of increased absorption, or an actual increase in UC luminescence due to an increased quantum yield. If the increase is mainly due to an absorption enhancement, the same overall effect can be achieved with a smaller amount of material. The overall impact on the system efficiency of an UC solar cell device, however, would be limited, as those devices are mostly limited by the low UC efficiency. Therefore, we calculated an estimate for how the quantum yield changes by
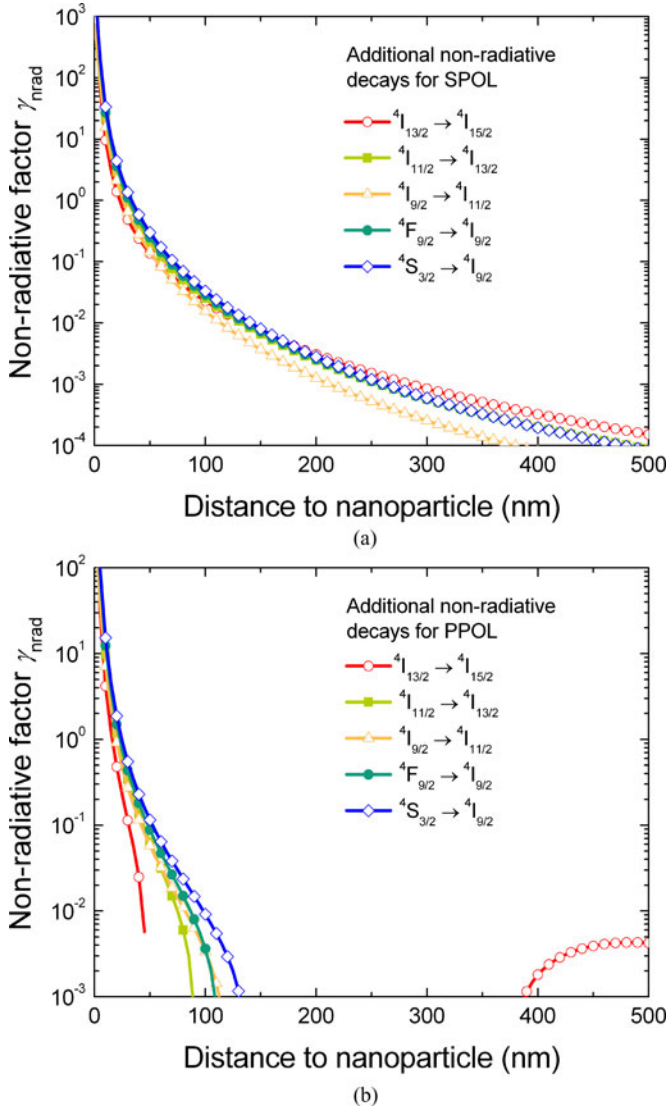
Fig. 6. Factor $\gamma_{\mathrm{nrad},i}$ that describes the additional nonradiative decay relative to the nonradiative decay without the nanoparticle for (a) SPOL and (b) PPOL. In particular close to the nanoparticle, there is significant additional nonradiative decay due to the nanoparticle.
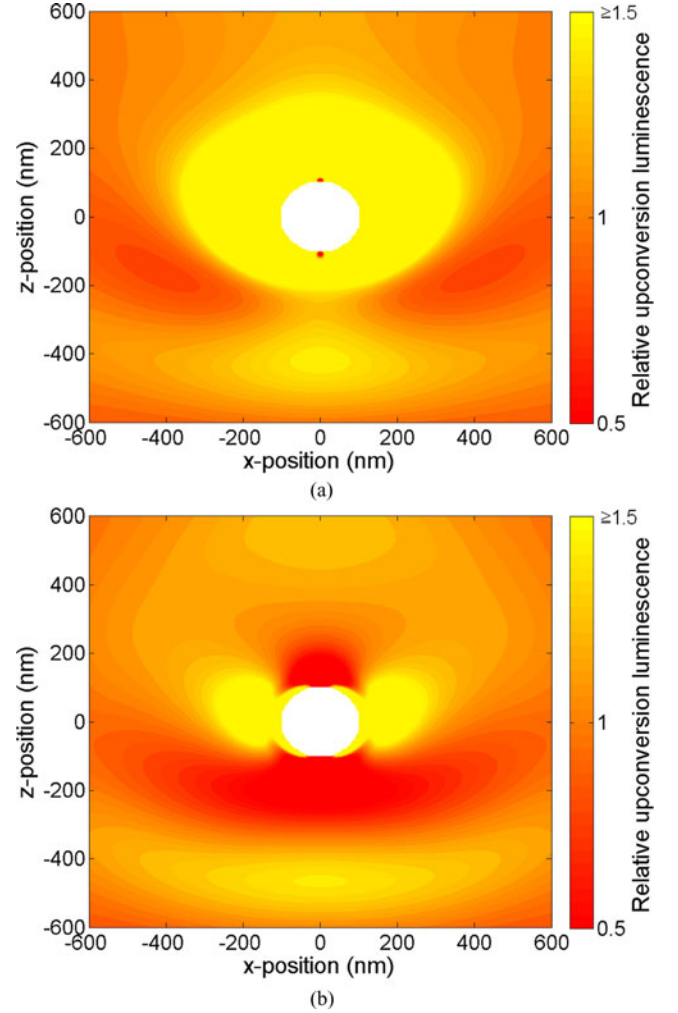

Fig. 7. Relative UC luminescence in proximity of a gold nanoparticle with 100-nm radius for the most important radiative transition from $^4I_{11/2}$ to $^4I_{15/2}$. The results are shown for the (a) polarization of the UC emission perpendicular to the particle's surface (SPOL) and for the (b) parallel polarization (PPOL). Regions of strong increase in luminescence but also with suppressed luminescence are visible. The direction of incidence of the exciting illumination at 1523 nm is from the bottom of the graphs (positive z-direction).
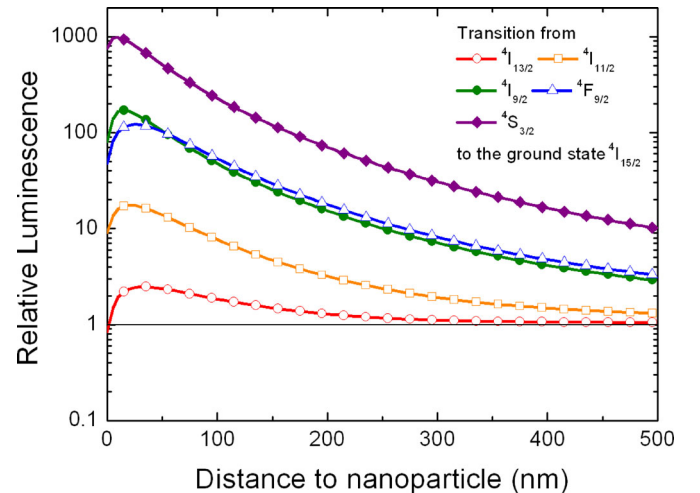

Fig. 8. Increase in UC luminescence at a certain distance to the gold nanoparticle for the weighted average of PPOL and SPOL. High enhancement factors are found, especially, for the higher energy transitions.

dividing the relative change in UC luminescence by the change of the absorption. The results of this analysis are shown in Fig. 9.

To calculate the presented dependence on the distance to the nanoparticle, the average over spherical shells surrounding the gold nanoparticle was taken. When calculating the overall average of the UC quantum yield change, the individual values were weighted with the distance dependent absorption values. For an exact analysis, the weighting needs to be performed with the absorption values of every point in the simulation volume. In this analysis, it can be seen that the increase in efficiency is considerably smaller than the overall change in UC luminescence. An overall enhancement of the UC quantum yield is only found for distances larger than 50 nm from the nanoparticle.
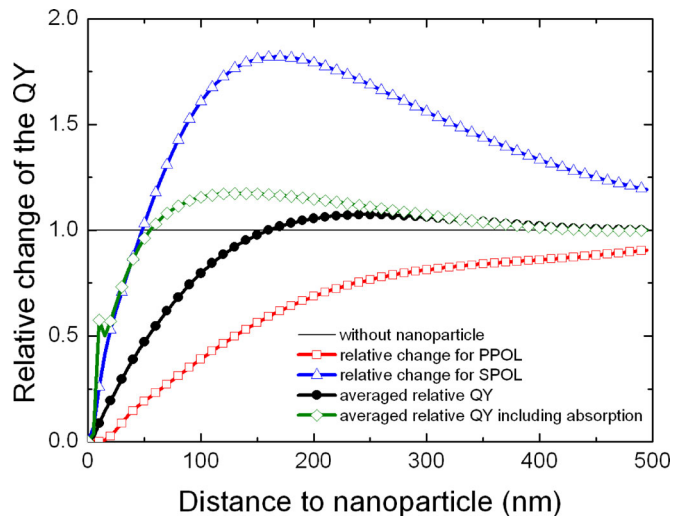
Fig. 9. Relative change of the UC quantum yield (QY) in dependence on the distance to the nanoparticle.

V. CONCLUSION

In this paper, we have reviewed recent results achieved with solar cell upconverter systems based on silicon solar cells and the upconverter material β-NaYF$_4$:20%Er^{3+}. Although the achieved efficiencies are relatively high in the context of UC for solar cells, the absolute impact on the overall efficiency of the solar cell is only very little. This motivates why additional means of increasing UC efficiency are necessary. We have shown that the plasmon resonance in gold nanoparticles has the potential to increase UC efficiency. We investigated in detail the impact of gold nanoparticles on UC by coupling a rate equation model that describes the upconverting material β-NaYF$_4$:20%Er^{3+} with Mie theory and exact electrodynamic theory calculations of the plasmon resonance in gold nanoparticles. It is important to consider the change of the local optical field intensities, the change in the transition rates within the upconverter, and the addition of nonradiative decay channels due to the nanoparticles and different polarization directions. We found that both UC luminescence and UC quantum yield can be increased when the upconverter is placed at a distance larger than 50 nm from the surface of a gold nanoparticle of 200-nm diameter. It remains to be investigated whether a higher increase in UC efficiency can be achieved with different nanoparticle sizes. The fact that higher energy transitions increase more strongly according to our model than the transitions most important for UC implies that the plasmon resonance could be tuned into a more favorable spectral region than achieved with the 200-nm particle. With triangular-shaped nanoparticles, it might be possible to achieve higher local field intensities, and with metal-coated dielectric nanoparticles, nonradiative processes might be reduced. With the complex model presented here, now a tool is available that allows one to evaluate the impact of such complex geometries on UC and to optimize them while taking into account all relevant processes.

REFERENCES

[1] F. Auzel, "Upconversion processes in coupled ion systems," *J. Luminescence*, vol. 45, pp. 341–345, 1990.

[2] T. Trupke, M. A. Green, and P. Würfel, "Improving solar cell efficiencies by up-conversion of sub-band-gap light," *J. Appl. Phys.*, vol. 92, pp. 4117–4122, 2002.

[3] J. F. Suyver, J. Grimm, M. K. van Veen, D. Biner, K. W. Krämer, and H. U. Güdel, "Upconversion spectroscopy and properties of NaYF$_4$ doped with Er^{3+}, Tm^{3+} and/or Yb^{3+}," *J. Luminescence*, vol. 117, pp. 1–12, 2006.

[4] B. S. Richards and A. Shalav, "Enhancing the near-infrared spectral response of silicon optoelectronic devices via up-conversion," *IEEE Trans. Electron Devices*, vol. 54, no. 10, pp. 2679–2684, Oct. 2007.

[5] S. Fischer, J. C. Goldschmidt, P. Löper, G. H. Bauer, R. Brüggemann, K. W. Krämer, D. Biner, M. Hermle, and S. W. Glunz, "Enhancement of silicon solar cell efficiency by upconversion: Optical and electrical characterization," *J. Appl. Phys.*, vol. 108, pp. 044912-1–044912-11, 2010.

[6] J. C. Goldschmidt, S. Fischer, P. Löper, K. W. Krämer, D. Biner, M. Hermle, and S. W. Glunz, "Experimental analysis of upconversion with both coherent monochromatic irradiation and broad spectrum illumination," *Solar Energy Mater. Solar Cells*, vol. 95, no. 7, pp. 1960–1963, 2011.

[7] J. Gersten and A. Nitzan, "Spectroscopic properties of molecules interacting with small dielectric particles," *J. Chem. Phys.*, vol. 75, pp. 1139–1152, 1981.

[8] G. Sun, J. B. Khurgin, and R. A. Soref, "Practicable enhancement of spontaneous emission using surface plasmons," *Appl. Phys. Lett.*, vol. 90, pp. 111107-1–111107-3, 2007.

[9] O. L. Muskens, V. Giannini, J. A. Sanchez-Gil, and J. Gamez Rivas, "Strong enhancement of the radiative decay rate of emitters by single plasmonic nanoantennas," *Nano. Lett.*, vol. 7, pp. 2871–2875, 2007.

[10] J. T. van Wijngaarden, M. M. van Schooneveld, C. de Mello Donegá, and A. Meijerink, "Enhancement of the decay rate by plasmon coupling for Eu 3+ in an Au nanoparticle model system," *EPL (Europhys. Lett.)*, vol. 93, p. 57005, 2011.

[11] P. Johansson, H. Xu, and M. Käll, "Surface-enhanced Raman scattering and fluorescence near metal nanoparticles," *Phys. Rev. B*, vol. 72, pp. 035427-1–035427-17, 2005.

[12] H. Mertens and A. Polman, "Plasmon-enhanced erbium luminescence," *Appl. Phys. Lett.*, vol. 89, pp. 1–3, 2006.

[13] F. Hallermann, C. Rockstuhl, S. Fahr, G. Seifert, S. Wackerow, H. Graener, G. von Plessen, and F. Lederer, "On the use of localized plasmon polaritons in solar cells," *Phys. Status Solidi A*, vol. 205, pp. 2844–2861, 2008.

[14] S. Schietinger, T. Aichele, H.-Q. Wang, T. Nann, and O. Benson, "Plasmon-enhanced upconversion in single NaYF4:Yb3+/Er3+ codoped nanocrystals," *Nano. Lett.*, vol. 10, pp. 134–138, 2009.

[15] S. Schietinger, M. Barth, T. Aichele, and O. Benson, "Plasmon-enhanced single photon emission from a nanoassembled metal–diamond hybrid structure at room temperature," *Nano. Lett.*, vol. 9, pp. 1694–1698, 2009.

[16] E. Verhagen, L. Kuipers, and A. Polman, "Field enhancement in metallic subwavelength aperture arrays probed by erbium upconversion luminescence," *Opt. Exp.*, vol. 17, pp. 14586–14598, 2009.

[17] R. Esteban, M. Laroche, and J. J. Greffet, "Influence of metallic nanoparticles on upconversion processes," *J. Appl. Phys.*, vol. 105, pp. 033107-1–033107-10, 2009.

[18] J. C. Goldschmidt, *Novel Solar Cell Concepts*. Munich, Germany: Verlag Dr. Hut, 2009.

[19] B. R. Judd, "Optical absorption intensities of rare-earth ions," *Phys. Rev.*, vol. 127, pp. 750–761, 1962.

[20] G. S. Ofelt, "Intensities of crystal spectra of rare-earth ions," *J. Chem. Phys.*, vol. 37, pp. 511–520, 1962.

[21] B. Henderson and G. F. Imbusch, *Optical Spectroscopy of Inorganic Solids* (Monographs on the Physics and Chemistry of Materials). Oxford, U.K.: Clarendon, 1989.

[22] M. J. Weber, "Probabilities for radiative and nonradiative decay of Er^{3+} in LaF$_3$," *Phys. Rev.*, vol. 157, pp. 262–272, 1967.

[23] S. Fischer, H. Steinkemper, P. Löper, M. Hermle, and J. C. Goldschmidt, "Modeling upconversion of erbium doped microcrystals based on experimentally determined Einstein coefficients," *J. Appl. Phys.*, vol. 111, no. 1, pp. 013109-1–013109-13, 2012.

[24] F. Hallermann, J. C. Goldschmidt, S. Fischer, P. Löper, and G. von Plessen, "Calculation of up-conversion photoluminescence in Er^{3+} ions near noble-metal nonoparticles," presented at Proc. Int. Soc. Opt. Eng., vol. 7725, Brussels, Belgium, 2010.

[25] C. F. Bohren and D. R. Huffman, *Absorption and Scattering of Light by Small Particles*. Hoboken, NJ: Wiley, 1983.

[26] K. Young Sik, P. T. Leung, and T. F. George, "Classical decay rates for molecules in the presence of a spherical surface: A complete treatment," *Surface Sci.*, vol. 195, pp. 1–14, 1988.

[27] F. Kaminski, V. Sandoghdar, and M. Agio, "Finite-difference time-domain modeling of decay rates in the near field of metal nanostructures," *J. Comput. Theor. Nanosci.*, vol. 4, pp. 635–643, 2007.

[28] H. Mertens, A. F. Koenderink, and A. Polman, "Plasmon-enhanced luminescence near noble-metal nanospheres: Comparison of exact theory and an improved Gersten and Nitzan model," *Phys. Rev. B*, vol. 76, pp. 115123-1–115123-12, 2007.

Authors' photographs and biographies not available at the time of publication.